

# Mechanisms of Antioxidant Action: Transformations Involved in the Antioxidant Function of Metal Dialkyl Dithiocarbamates. III

S. AL-MALAIKA, A. MAROGI, and G. SCOTT, *Department of  
Molecular Sciences, Aston University, Aston Triangle, Birmingham  
B4 7ET, United Kingdom*

## Synopsis

The behaviors of iron, nickel, and zinc dialkyl dithiocarbamates were compared with the corresponding thiuram disulphide in their reaction with cumene hydroperoxide (CHP) at 110°C. The metal complexes exhibit both homolytic and heterolytic processes and transformation products formed during the above reactions and not the initial metal complexes were found to be responsible for the heterolytic decomposition process. However, the nature of the initial transformation products in the case of the iron and nickel complexes differed from those of the corresponding zinc complex. In the former case the corresponding disulfide was shown to be the initial transformation product while there was no evidence for the formation of disulfide in the case of the zinc complex. This difference appears to be responsible for the observed different kinetic behavior of CHP decomposition in the presence of the nickel and iron complexes from that in the presence of zinc. This thiuram disulfide behaves quite differently from the metal complexes in that heterolytic decomposition of hydroperoxide predominates at all molar ratios of the disulphide to the CHP. The hydroperoxide decomposition curves in this case show only one step in contrast to the metal complexes which show a multistep behavior, and this was shown to correspond to the third catalytic stage in the reaction of the metal complexes. Comparison of the rate constant of this step with that of the final step of the metal complexes shows a close resemblance to the case of the iron and nickel and is quite different from that of the zinc complex, confirming the intermediacy of the disulfide in the former cases but not in the latter.

## INTRODUCTION

It has been shown that metal dialkyl dithiocarbamates (MDRC) act as antioxidants for polymers partly by destroying hydroperoxides<sup>1-3</sup> and partly, by scavenging radicals.<sup>2,4</sup> Different metal dialkyl dithiocarbamates (e.g., nickel, zinc, and iron), however, have different stabilization roles in polyolefins, and these in turn differ from that of the thiuram disulfides. While nickel and zinc dialkyl dithiocarbamates (MDRC, M = Ni, Zn) are used in industry as thermal and photo antioxidants,<sup>5</sup> the iron complex is used as a prooxidant under photooxidative conditions in spite of the fact that it is a very effective melt stabilizer for polyolefins.<sup>6,7</sup> The behavior of the tetraalkyl thiuram disulfides (TRTD), on the other hand, resemble the disulfides of other dithioic acids (e.g., disulfides of dithiophosphoric and xanthic acids) in that their photoantioxidant effect increases markedly in polyolefins which have been subjected to oxidative processing in the melt.<sup>8</sup> Moreover, the difference in behavior of the different metal complexes and their corresponding disulfides was exploited in

developing a very effective time-controlled stabilizer system for polyolefines based on combinations of these different compounds.<sup>6,9</sup>

In parts I and II,<sup>2,3</sup> we investigated the nature of intermediates involved in the antioxidant behavior of a zinc dialkyl dithiocarbamate. The purpose of the present investigation is to compare, under similar experimental conditions, the antioxidant mechanisms of iron and nickel dithiocarbamates with that of the zinc complex and to examine the mechanisms of the thiuram disulphide and its relevance to that of the metal complexes.

## EXPERIMENTAL

### Materials

Zinc diethyl dithiocarbamate (ZnDEC) was supplied by Robinson Brothers Ltd. Nickel diethyl dithiocarbamate (NiDEC) and iron dimethyl dithiocarbamate (FeDMC) were prepared by double decomposition of a 10% solution of the corresponding sodium salts (ex. Robinson Brothers) with a saturated solution of the transition metal chlorides. All metal dithiocarbamates were recrystallized from benzene. Tetraethyl thiuram disulfide (TETD) was prepared as follows: 0.02 mol of iodine solution (in methanol) was added dropwise with continuous stirring to 0.02 mol of sodium diethyl dithiocarbamate in water. A pale yellow precipitate appeared during the addition of the iodine solution (the addition of iodine was stopped when the iodine color started to appear; this was followed by addition of few drops of the sodium salt to neutralize any excess iodine). The solution was filtered off and the precipitate was washed several times with water before drying in a vacuum oven at room temperature. The precipitate (TETD) was recrystallized from hexane. Melting points and elemental analysis of all the compounds prepared here are shown in Table I.

Cumene hydroperoxide (CHP) (ex. BDH) was purified via its sodium salt by the method of Kharash et al.<sup>10</sup> Cumene (technical grade, BDH) was washed four times with concentrated sulfuric acid, followed by water, 10% sodium carbonate solution, and finally with water. After thorough drying with mag-

TABLE I  
Elemental Analysis, Color, and Melting Points for Dithiocarbamates

Compound	Color	Melting Point (°C)	C%	H%	N%	S%	
TETD	Pale yellow	70	40.70	7.00	9.20	43.40	Found
			40.54	7.79	9.46	43.24	Calcd.
ZDEC	White	170	33.20	5.70	8.30	36.10	Found
			33.09	5.55	7.90	35.34	Calcd.
NDEC	Green	225	34.00	5.50	7.64	36.40	Found
			33.80	5.67	7.88	36.10	Calcd.
FDMC	Black	> 300	25.60	4.40	10.10	45.00	Found
			25.90	4.35	10.04	46.00	Calcd.

nesium sulfate, the product was distilled from phosphorous pentoxide under nitrogen and used.

### Thermal Decomposition of CHP and Product Analysis

In a specially designed reaction cell fitted with a condenser, chlorobenzene was introduced and allowed to equilibrate for 5 min in a thermostated oil bath at  $110 (\pm 0.5^\circ\text{C})$ . A calculated amount of CHP was added and allowed a further 5 min to equilibrate under a slow steady stream of nitrogen which ensures purging and efficient mixing. The additive was introduced quickly and sampling of the reaction mixture was commenced 5 min later. Iodometric titration was used for following the CHP decomposition in the presence and absence of the antioxidant.

Products obtained from the above thermal studies were analyzed by GLC using Pye Unicam GCD chromatograph with flame ionization detector and a 2-m glass column packed with poly(ethylene glycol) adipate on chromosorb W. Best separation was achieved by a temperature programme (initial temperature  $85^\circ\text{C}$  held for 1 min after which the temperature was increased at a rate of  $8^\circ\text{C}/\text{min}$  until a final temperature of  $150^\circ\text{C}$  was attained). When product distributions during reactions of dithiocarbamates with CHP were studied, the undecomposed hydroperoxide (present in samples taken-out during early stages of the reactions before complete decomposition of CHP) was reduced to  $\alpha$ -cumyl alcohol by addition of excess triphenyl phosphine before the sample was analyzed by GLC. Blank reactions between triphenyl phosphine and different concentrations of CHP were used, and their GLC was run to generate a calibration curve which relates the quantity of  $\alpha$ -cumyl alcohol derived from the phosphine reduction of hydroperoxide and the CHP concentration and hence an accurate assessment of the concentration of  $\alpha$ -cumyl alcohol present in the test samples before addition of phosphine was possible. Oxygen absorption studies were carried out as described previously.<sup>11</sup>

## RESULTS

### Reactions of MDRC with CHP and Their Product Analysis

The kinetics of the decomposition of cumene hydroperoxide (CHP) at  $110^\circ\text{C}$  in the presence of ZnDEC at different  $[\text{CHP}]/[\text{ZnDEC}]$  molar ratios have been investigated previously.<sup>2</sup> Figures 1 and 2 show the behavior of NiDEC and FeDMC under the same conditions in which the concentration of the CHP was kept constant while varying the concentration of the metal complex. Figure 3 compares the behavior of the above metal complexes with that of the ZnDEC at  $[\text{CHP}]/[\text{MDRC}]$  molar ratio of 30. It is clear that both NiDEC and FeDMC behave similarly, but quite differently from the zinc complex. The decomposition curves of the iron and nickel complexes (at ratios  $> 20$ ) (see Figs. 1 and 2) show a typical three-step behavior; a first rapid initial catalytic stage followed by an induction period which leads into a slower first-order catalytic reaction, which was also observed in the case of nickel dithiophosphates and xanthates.<sup>12</sup> By contrast, the zinc complex<sup>2</sup> does not show the initial rapid first stage. However, at a stoichiometric  $[\text{CHP}]/[\text{MDRC}]$  ratio, only the first stage of the decomposition of CHP

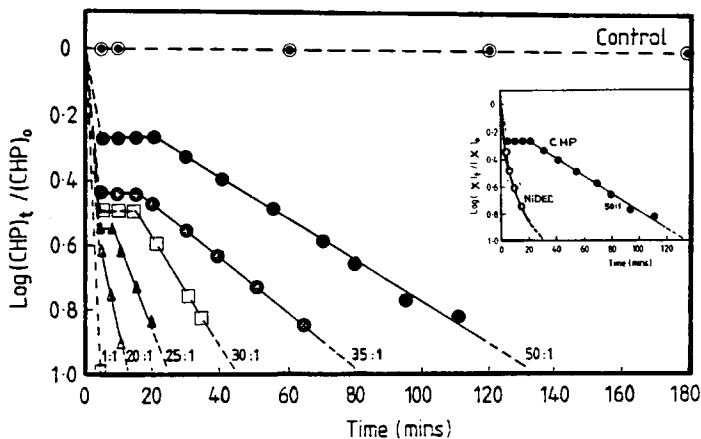


Fig. 1. Decomposition of CHP ( $1 \times 10^{-2}M$ ) in chlorobenzene at  $110^\circ C$  by NiDEC, at different molar ratios of  $[CHP]/[NiDEC]$ . Inset reproduces the 50:1 peroxide decomposition curve and shows the associated decay of the NiDEC uv absorbance.

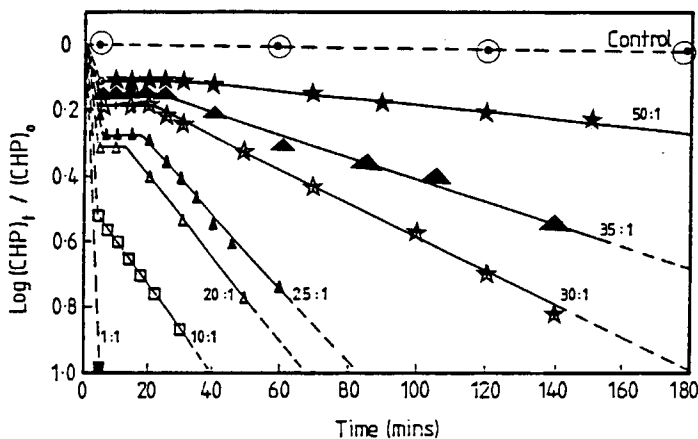


Fig. 2. Decomposition of CHP ( $1 \times 10^{-2}M$ ) in chlorobenzene at  $110^\circ C$  by FeDMC, at different molar ratios of  $[CHP]/[FeDMC]$ .

occurs in the presence of NiDEC and FeDMC (see Figs. 1 and 2). The length of the second stage induction period increases with increasing  $[CHP]/[MDRC]$  molar ratio (i.e., with decreasing metal complex concentration) whereas the second catalytic stage becomes slower (Fig. 4) under these conditions. This behavior is the exact opposite of what happens in the case of the zinc complex (see Fig. 4). These results suggest formation of a stable intermediate in the case of FeDMC and NiDEC. TLC studies (see Fig. 5) show this to be the disulfide which is formed in the rapid first stage. It has been shown that for zinc dithiocarbamate the length of the induction period varies linearly with concentration whereas the rate of the second catalytic stage is proportional to the concentration,<sup>2</sup> suggesting that the nature of the intermediate product(s)

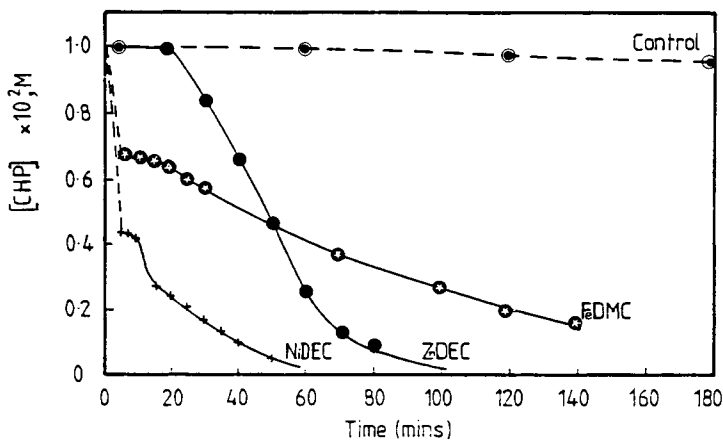


Fig. 3. Comparison of CHP decomposition curves for reactions of MDRC, (M = Fe, Ni, Zn) with CHP in chlorobenzene at 110°C and a molar ratio of  $[\text{CHP}]/[\text{MDRC}] = 30$ .

must be different in this case. We have previously prepared an authentic sample of zinc dithioperthiocarbamate (ZnDMSO) and have shown that it is the first oxidation product to be formed from ZnDRC during its reaction with hydroperoxides.<sup>3</sup> However, neither the corresponding dithioperthiocarbamate complexes of nickel and iron nor the thiol-sulfinate derived from these complexes could be isolated, indicating their labile nature.

In the case of nickel complexes of other dithioic acids, e.g., dithiophosphates and xanthates, the first transformation product was found to be the corresponding disulfide which forms during the first few minutes of their reactions with hydroperoxides and subsequently disappears.<sup>12</sup> The possibility of forming thioram disulfides during reactions of metal dithiocarbamates with hydroperoxides was therefore examined. TLC analysis of samples taken during reaction (in chlorobenzene at 110°C) of MDRC (M = Zn, Ni, Fe) with CHP at a molar  $[\text{CHP}]/[\text{MDRC}]$  ratio of 50 (Fig. 5) shows clearly that in the case of both the nickel and the iron complexes the corresponding disulfide is formed in the first 3 min of the reaction but disappears completely at the end of the reactions. The zinc complex, on the other hand, did not form a disulfide at any stage. These observations were confirmed using the diagnostic tellurium powder test for thioram disulfides<sup>13</sup>: both NiDEC and FeDMC after 3 min reaction gave an immediate brick-red color on addition of tellurium powder, confirming the formation of the divalent tellurium dithiocarbamate. Repetition of the test after a further 7 min gave negative results, indicating that the disulfide had disappeared via its conversion to perhaps further sulfur acids. Results from the zinc complex were negative throughout the reaction.

Product distribution curves and the corresponding peroxide decomposition curves of the nickel and iron complexes at molar  $[\text{CHP}]/[\text{MDRC}]$  ratio of 30 (at 110°C) are compared in Figures 6 and 7. In both cases, at the beginning of the reactions free radical products (acetophenone and  $\alpha$ -cumyl alcohol) form rapidly with the formation of only small amount of the ionic product, phenol. However, towards the end of the induction period the concentration of

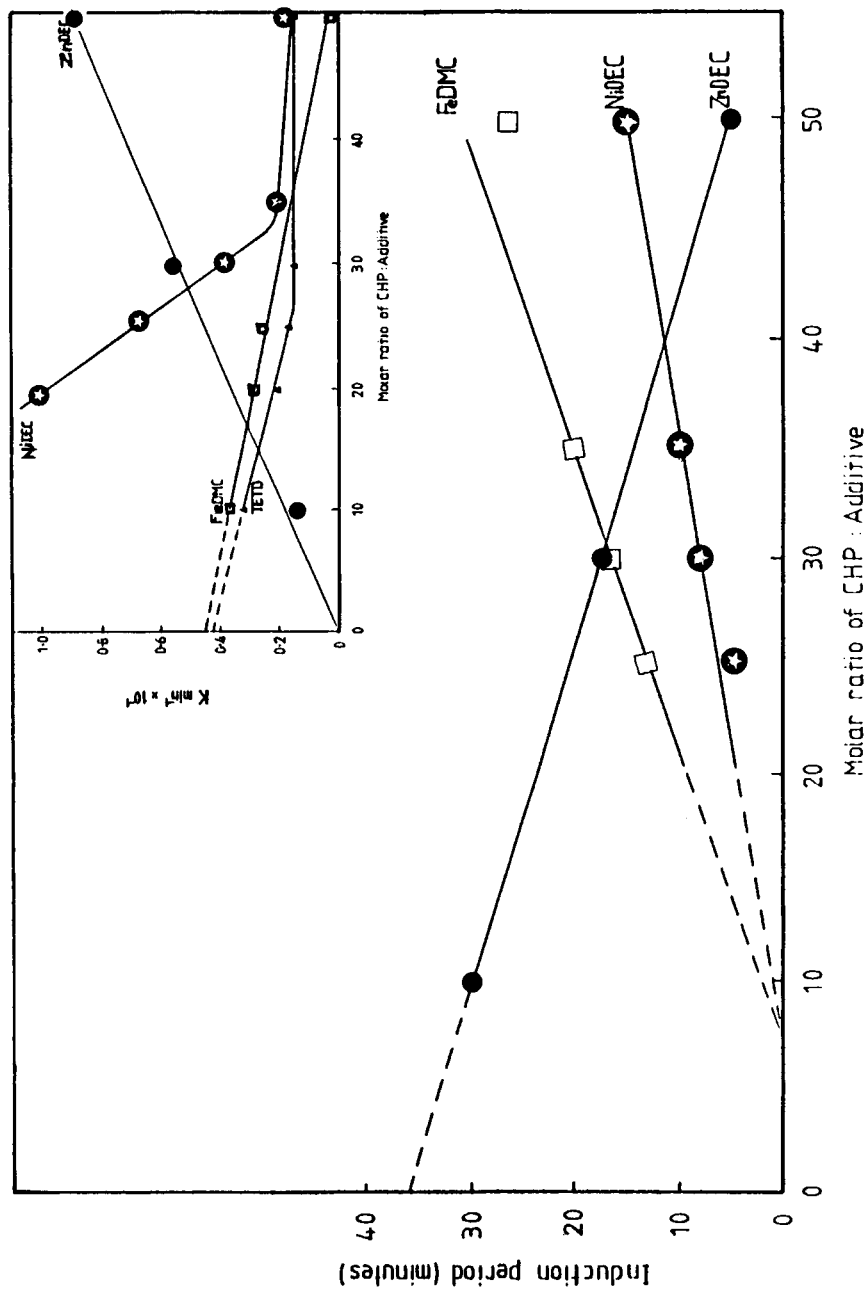


Fig. 4. Changes in induction period of CHP decomposition curves of MDRC, (M = Fe, Ni, Zn) and the rate constant of the second catalytic stage in these curves (inset) as a function of  $[CHP]/[MDRC]$  molar ratios. The concentration of CHP in all curves was  $1 \times 10^{-2}M$ .

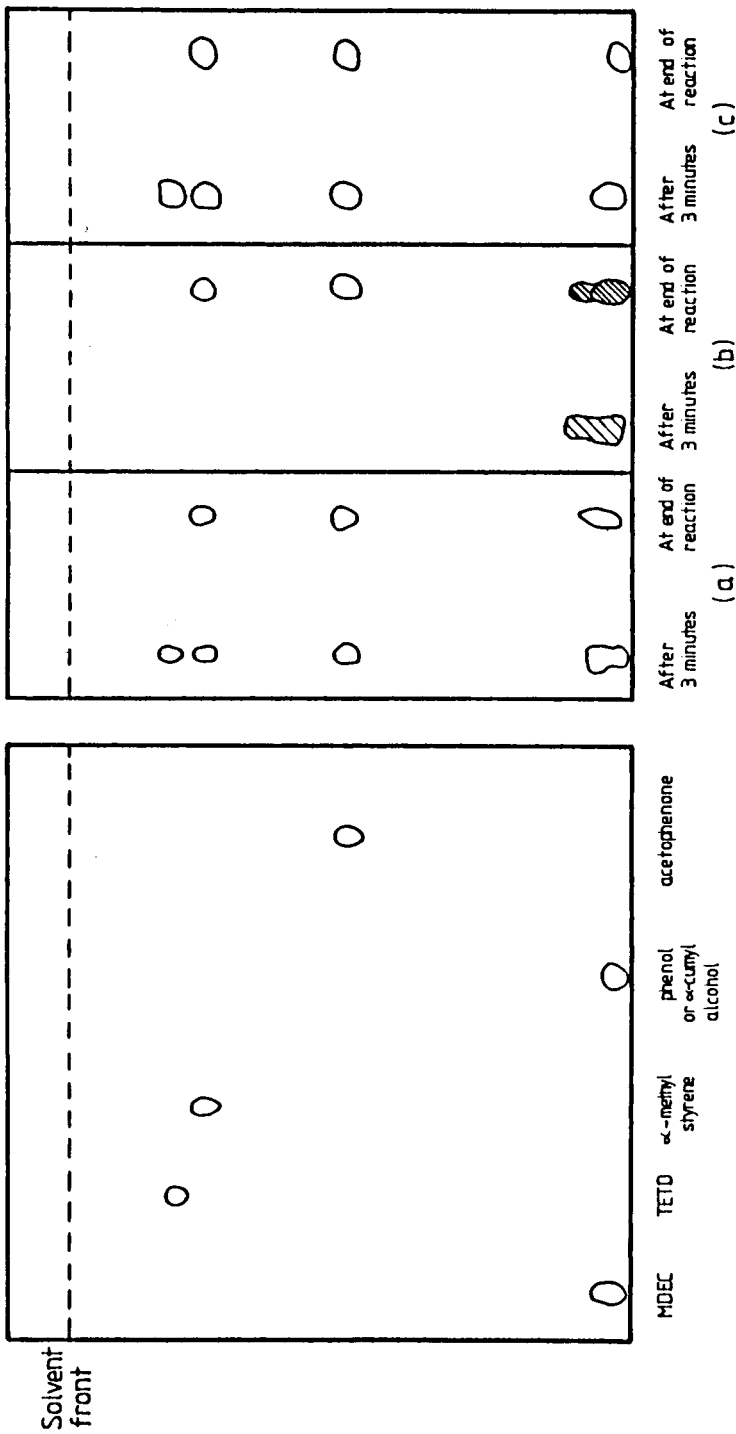


Fig. 5. Thin layer chromatograms of products formed during reactions of CHP ( $1 \times 10^{-2}M$ ) with NiDEC and FeDMC (a), ZnDEC (b), and TETD (c) at  $110^\circ C$ . Concentration of all MDRC =  $2 \times 10^{-3}M$ .

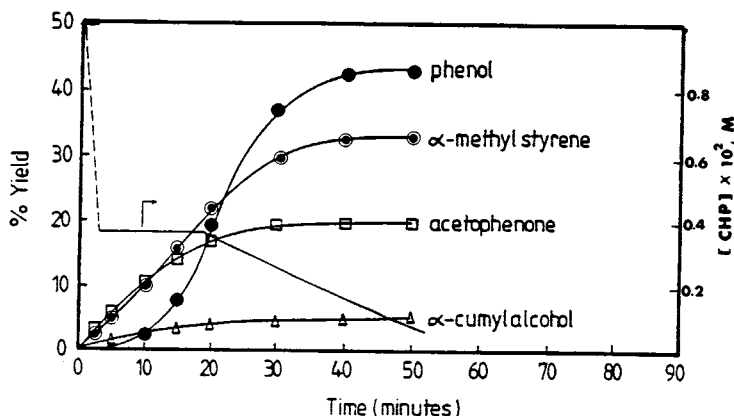
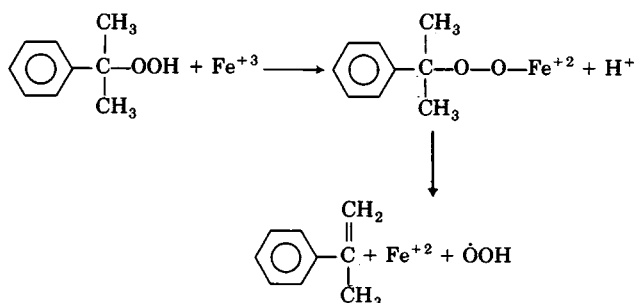


Fig. 6. Product distribution (by GLC) obtained from a reaction of CHP ( $1 \times 10^{-2}M$ ) and NiDEC in chlorobenzene at  $110^\circ C$  and a molar ratio  $[CHP]/[NiDEC] = 30$ . The corresponding CHP decomposition curve is also shown.

acetophenone and  $\alpha$ -cumyl alcohol start to level off while phenol builds up rapidly, indicating the predominance of an ionic process at the end of these reactions. The high concentration of  $\alpha$ -methyl styrene at the end of these reactions suggests that the acidic species responsible for the formation of phenol also cause dehydration of  $\alpha$ -cumyl alcohol to the corresponding olefin, in a way similar to that observed for the zinc complex.<sup>2</sup> It is also clear from Figures 6 and 7 that  $\alpha$ -methyl styrene also forms rapidly at the beginning of the reaction (before the end of the induction period), and this is more pronounced in the case of the FeDMC. A free radical reaction must also lead to  $\alpha$ -methyl styrene, possibly by breakdown of an intermediate iron hydroperoxide complex formed in the redox decomposition of CHP.



Figures 8 and 9 record the formation of final products of CHP decomposition by NiDEC and FeDMC (at  $110^\circ C$ ) at various  $[CHP]/[MDRC]$  molar ratios. It is clear that at lower molar ratios (near to stoichiometric) a homolytic free radical process predominates, as reflected by the high concentration of  $\alpha$ -cumyl alcohol and acetophenone, while at higher catalytic ratios the products



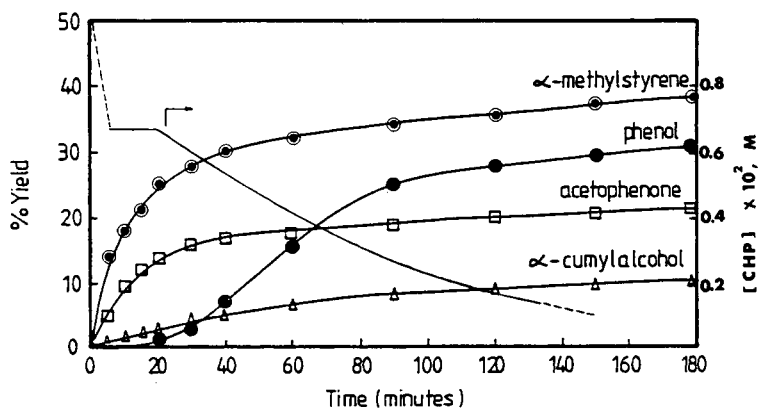


Fig. 7. Product distribution (by GLC) obtained from a reaction of CHP ( $1 \times 10^{-2} M$ ) and FeDMC in chlorobenzene at  $110^\circ C$  and a molar ratio  $[CHP]/[FeDMC] = 30$ . The corresponding CHP decomposition curve is also shown.

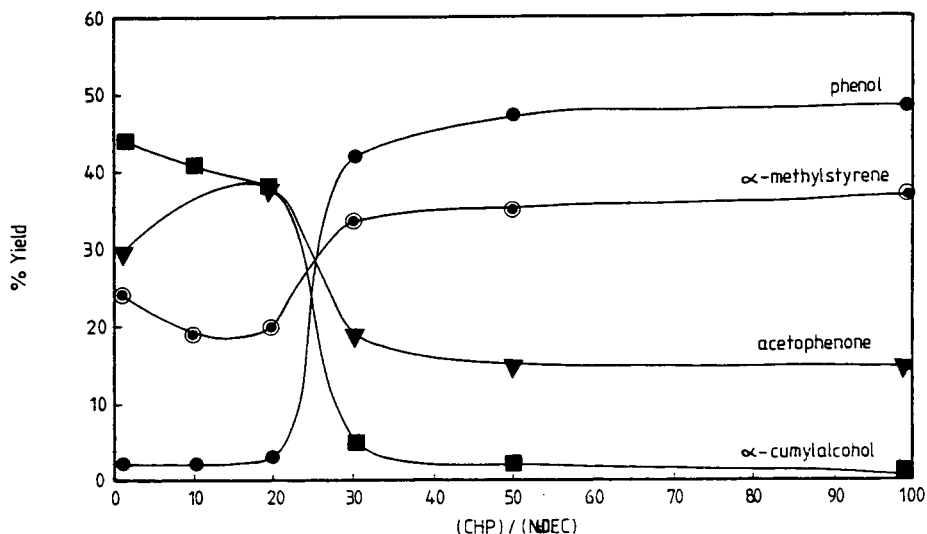


Fig. 8. Product yield after complete reaction of NiDEC with CHP at  $110^\circ C$  in chlorobenzene at various molar ratios of  $[CHP]/[NiDEC]$ .

formed are mainly those expected by a heterolytic ionic process. The presence of a constant but low proportion of the homolytic decomposition products at higher ratios indicates that the radical process makes a contribution in the overall mechanism at all ratios.

#### Reactions of TETD with CHP and Product Analysis

Reactions of TETD with CHP at  $110^\circ C$  and at different molar ratios (under conditions similar to those used for the nickel and iron complexes) were

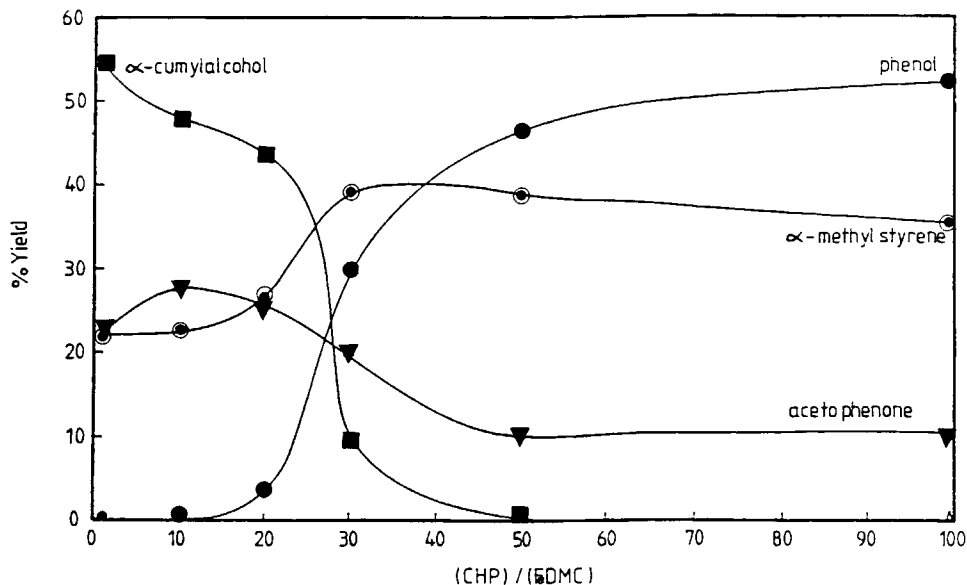


Fig. 9. Product yield after complete reaction of FeDMC with CHP at 110°C in chlorobenzene at various molar ratios of [CHP]/[FeDMC].

examined (Fig. 10). The decomposition curves here show only one step whereby the peroxide decomposes slowly and gradually in a way very similar to the slow second catalytic stage of FeDMC and NiDEC (see Figs. 1 and 2). The complete absence of the first rapid decomposition stage and the absence of an induction period in the case of the disulphide suggest that these two stages must be associated with the metal complexes only. During these two stages

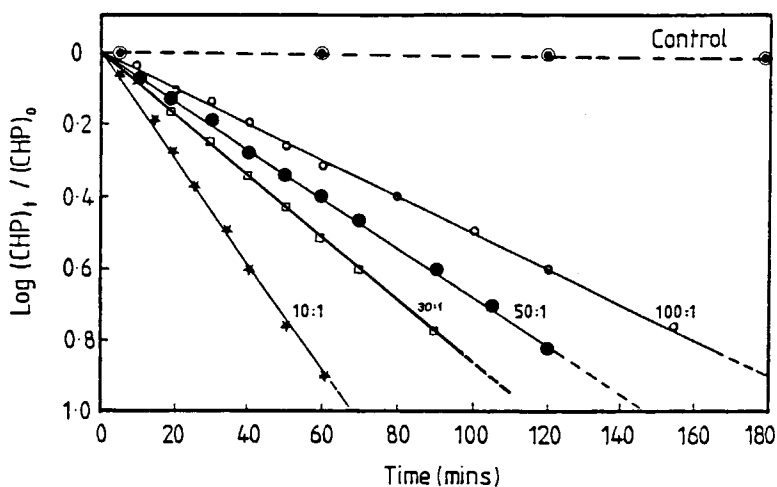


Fig. 10. Decomposition of CHP ( $1 \times 10^{-2}M$ ) in chlorobenzene at 110°C by TETD, at different molar ratios of [CHP]/[TETD].

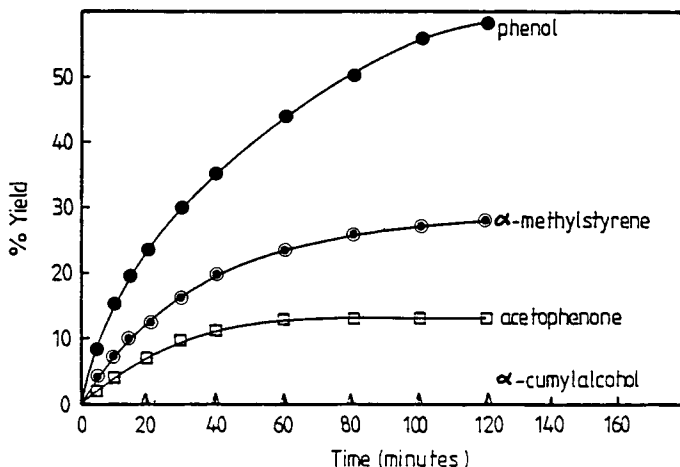


Fig. 11. Product distribution (by GLC) obtained from a reaction of CHP ( $1 \times 10^{-2}M$ ) and TETD in chlorobenzene at  $110^{\circ}C$  and a molar ratio  $[CHP]/[TETD] = 30$ .

the metal complexes ( $M = Ni, Fe$ ) oxidize initially to the corresponding disulphide (see Fig. 5) and subsequently to further oxidation products in a free radical generating process (see Figs. 6 and 7, in both cases acetophenone and  $\alpha$ -cumyl alcohol are the main products at the beginning of the reaction). In the case of the disulfide the one step decomposition curves (Fig. 10) must correspond to the third step (i.e., the second catalytic stage) in the decomposition curves of NiDEC and FeDMC. Figure 11 confirms this and shows that phenol, the ionic product, predominates from the beginning of the reaction of TETD with CHP at a  $[CHP]/[TETD]$  ratio of 30; a situation which is very different from the early stages of the reactions of the nickel and iron complexes with CHP but very similar to the third stage during which phenol builds up rapidly at the expense of the other products of the homolytic process. This observation lends further support for the postulate that the disulfide is the initial transformation product formed in the first stage during the reaction of NiDEC and FeDMC with hydroperoxides<sup>12,14</sup> and it is its further oxidation products which then trigger off the second catalytic stage in a way similar to the decomposition of the disulfide itself. There is, however, a striking difference in the mechanism of action of the disulphide and that of the nickel and iron complexes at low  $[CHP]/[dithiocarbamate]$  ratios (near to 1 : 1 molar). Figure 12 compares product distribution curves of the reaction of TETD with CHP at a  $[CHP]/[TETD]$  ratio of 10 (at  $110^{\circ}C$ ) with those of the iron and nickel complexes under the same conditions. At this molar ratio, products formed from the metal complexes are mainly those expected on the basis of a radical mechanism (acetophenone and  $\alpha$ -cumyl alcohol) while ionic products (phenol and  $\alpha$ -methyl styrene) predominate in the case of the disulphide. The dominating influence of the ionic reaction over the free radical process in the case of the disulfide was found to hold at all the molar ratios studied here including the stoichiometric ratio (Fig. 13).

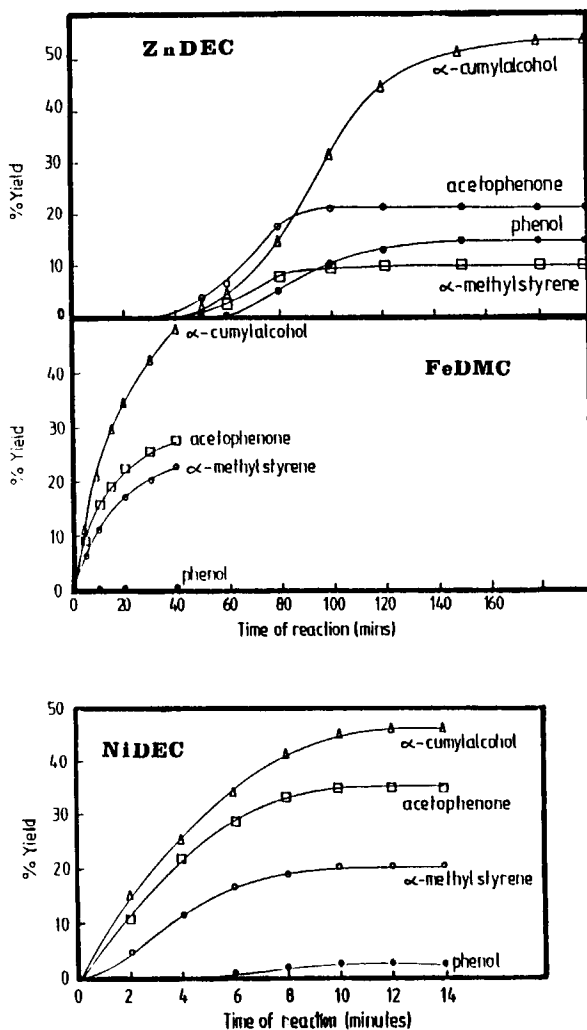


Fig. 12. Comparison of product distribution (by GLC) obtained from reactions of CHP ( $1 \times 10^{-2}M$ ) and MDEC ( $M = Fe, Ni, Zn$ ) in chlorobenzene at  $110^\circ C$  and a molar ratio  $[CHP]/[MDEC] = 10$ .

### Oxidation of Cumene in the Presence of Dithiocarbamates Initiated by AIBN and CHP and the Effect of Different Retarders

Figure 14 compares the behavior of the metal complexes ( $M = Zn, Ni, Fe$ ) and their corresponding disulfide (TETD) in cumene oxidation initiated by AIBN and by CHP. In the case of AIBN-initiated oxidation all the metal complexes show a short initial induction period, the length of which depends on the nature of the metal center. TETD, on the other hand, did not show any induction period and was a weaker inhibitor than the metal complexes. Figure 14 (inset) shows clearly that, although all the dithiocarbamates tested here have weak radical scavenging ability, the disulfide is almost inactive. The

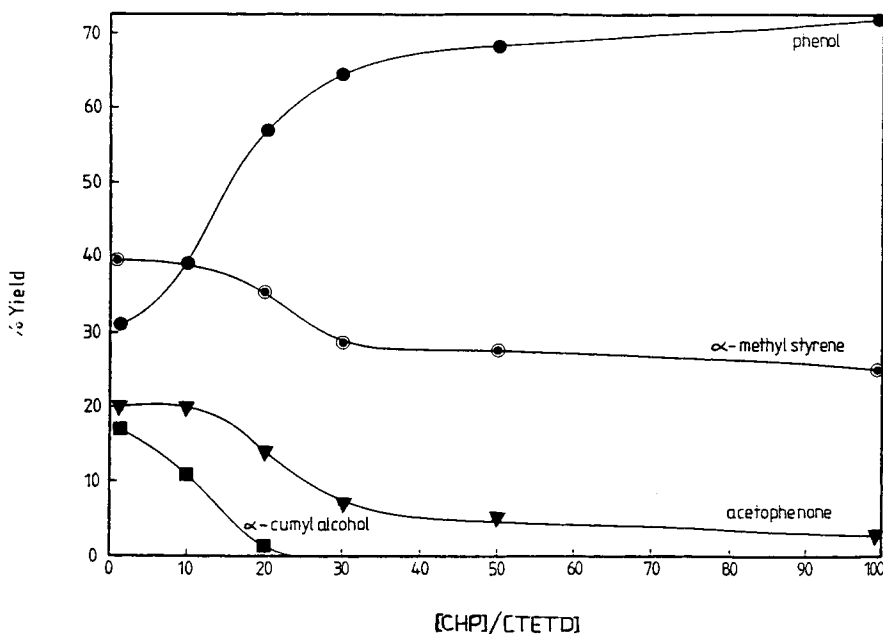


Fig. 13. Product yield after complete reaction of TETD with CHP ( $1 \times 10^{-2}M$ ) at  $110^\circ C$  in chlorobenzene at various molar ratios of  $[CHP]/[TETD]$ .

nickel complex shows the best performance when compared to the other two metal complexes. The behavior of the metal complexes in the autooxidation of cumene initiated by CHP (Fig. 14) is very different. NiDEC and FeDMC show a very similar behavior to that recently reported<sup>2</sup> in the case of the zinc (reproduced here), where there is an initial prooxidant effect, followed by complete inhibition of oxidation. The prooxidant effect observed during the early stages of the hydroperoxide-initiated oxidation again confirms that the main species responsible for the nonradical decomposition of CHP are not the metal complexes themselves but products of its oxidation by hydroperoxide. This was confirmed by showing that the nickel and iron dithiocarbamates had disappeared completely (see, for example, inset of Fig. 1 for NiDEC) by the end of the first step in their peroxide decomposition curves (i.e., well before the onset of the second ionic nonradical step).

It has been shown previously<sup>1</sup> that the main catalysts produced at the later stages of reactions of metal dithiolates and other related sulfur-containing compounds with hydroperoxides are sulfur acids, irrespective of the nature of the initial transformation products. The effect of a strong base on the autooxidation of cumene initiated by CHP in the presence of the three metal complexes was therefore examined. Figure 15 (inset) shows the effect of adding pyridine to the above reaction in the presence of MDRC ( $M = Ni, Fe, Zn$ ). It is clear that the antioxidant function of these complexes (see Fig. 14) is completely removed by pyridine confirming the important role of acidic species in these reactions. It has been suggested previously<sup>15</sup> that the main acidic species is almost certainly  $SO_3$ . A molecular sieve was therefore used in the above reactions in order to trap any trace of the gas, if formed. Figure 15

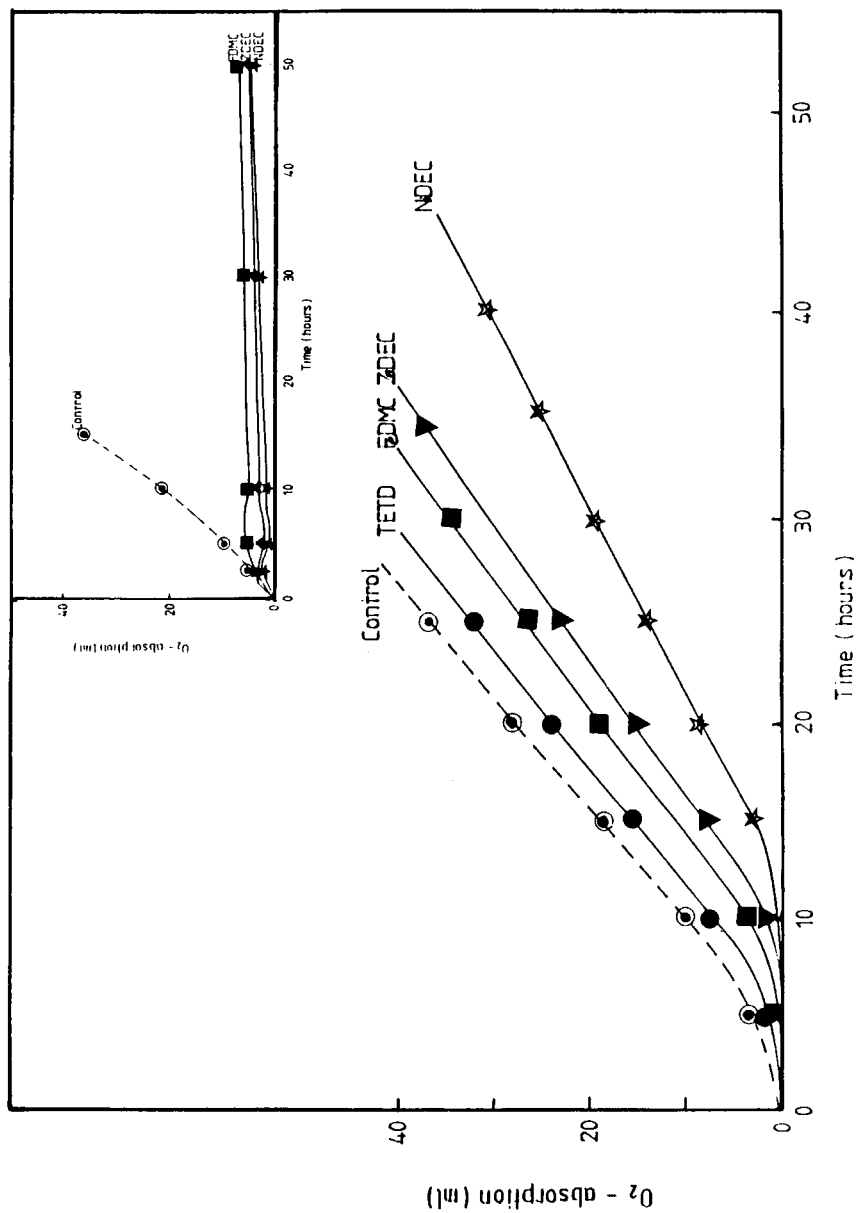


Fig. 14. Effect of dithiocarbamates ( $5 \times 10^{-5} M$ ) on the oxidation of cumene in the presence of AIBN ( $1 \times 10^{-2} M$ ) at  $50^\circ C$ . Inset shows the effect of the additives ( $5 \times 10^{-5} M$ ) on oxidation of cumene in the presence of CHP ( $1 \times 10^{-2} M$ ) at  $110^\circ C$ .

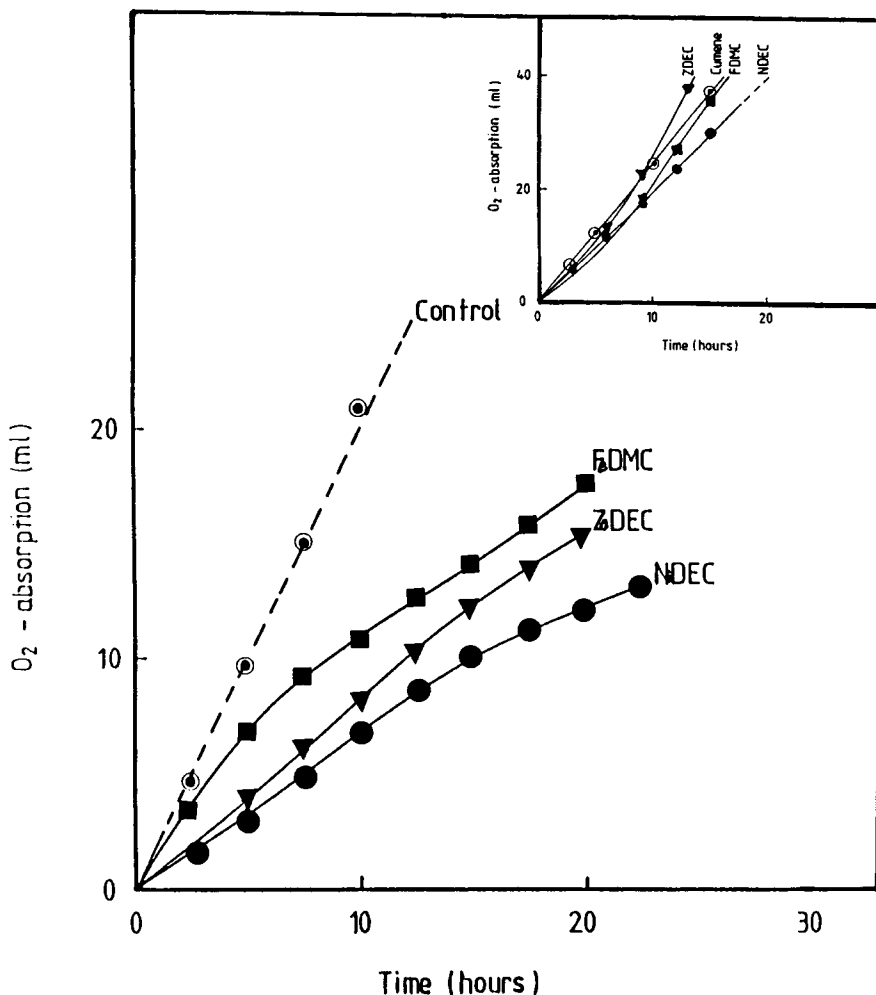


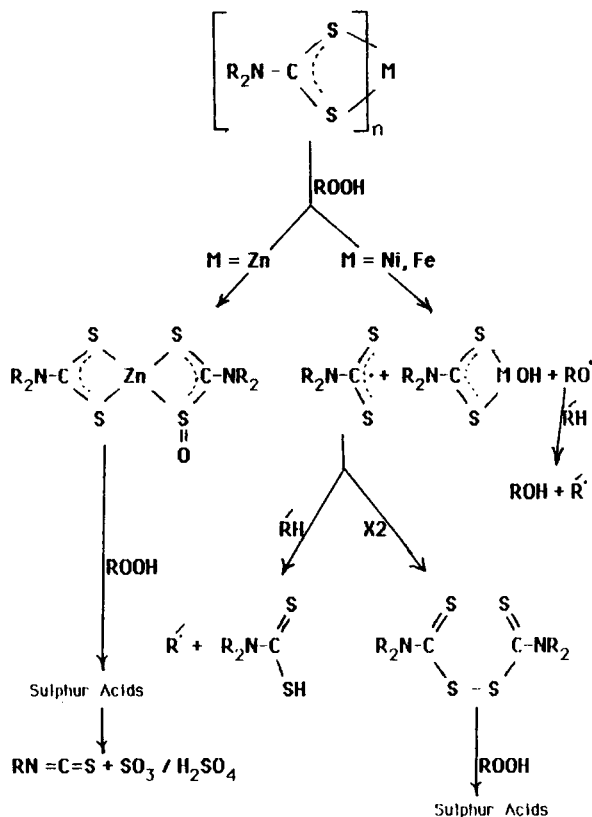
Fig. 15. Effect of molecular sieve (5A), and pyridine,  $5 \times 10^{-5}M$  (inset), on the oxidation of cumene in the presence of dithiocarbamates ( $5 \times 10^{-5}M$ ) and CHP (0.1M).

shows clearly that under these conditions the antioxidant activity is only partially removed. This suggests that other acid catalysts beside  $SO_3$  may be involved in the antioxidant action of metal dithiocarbamates. A likely explanation, however, is that  $H_2SO_4$ , formed by reaction of  $SO_3$  with water formed from the dehydration of  $\alpha$ -cumyl alcohol may be the residual non-volatile acid catalyst.

## DISCUSSION

The overall mechanisms of action of nickel, iron, and zinc dithiocarbamates are similar. Both homolytic and heterolytic processes are involved in all three, the importance of each depends on the  $[CHP]/[MDRC]$  ratio (see, for example, Fig. 8). In each case, the metal complexes themselves are not responsible for the heterolytic decomposition of hydroperoxides but rather

their transformation products which are formed by oxidation in the presence of hydroperoxides. This behavior is similar to that of other dithiolate metal complexes.<sup>1</sup> However, the nature of the initial transformation product(s) formed from the three complexes is quite different. This, in turn, leads to different kinetics of the decomposition curves at different [CHP]/[MDRC] molar ratios (Fig. 4). The nickel and iron dithiocarbamates form the corresponding disulfide (TRTD) as their initial oxidation product (Fig. 5). This is analogous to the formation of the corresponding disulphides from many other related sulfur-containing compounds such as mercaptobenzthiazole and its metal complexes, metal complexes of other dithioic acids such as dithiophosphoric and xanthic acids and mercaptothiazolines during similar high temperature reactions with hydroperoxides.<sup>1,16</sup> The behavior of the zinc dithiocarbamate, however, is quite different in that it does not form the disulfide at any stage of its reaction with hydroperoxides (see Fig. 5 and the negative tellurium test throughout its reaction). It was shown previously<sup>2</sup> that the thiopercarbamate (ZnDRSO) is the main initial transformation product in this case (see Scheme 1 below). The ease of formation of the initial transformation product, whether it is the disulfide or the dithiopercarbamate, may depend on the oxidizability of the central metal ion (NiDEC undergoes oxidation much more readily than ZnDEC<sup>17</sup>). The different mechanisms of action of the three metal complexes are summarized in Scheme 1.



Scheme 1. Proposed mechanisms of antioxidant action of MDRC



The thiuram disulfide shows quite a different overall mechanism of action. The free radical scavenging ability of the disulfide is minimal under the experimental conditions examined and phenol (the ionic product) remains the major decomposition product at all molar ratios. The metal complexes, on the other hand, act mainly by a free radical process at low molar ratios (Fig. 12)

### References

1. S. Al-Malaika, K. B. Chakraborty and G. Scott, in *Developments in Polymer Stabilization*—6, G. Scott, Ed., Applied Science, London, 1983, Chap. 3.
2. S. Al-Malaika, A. Marogi, and G. Scott, *J. Appl. Polym. Sci.*, **30**, 789 (1985).
3. S. Al-Malaika, A. Marogi, and G. Scott, *Polym. Deg. Stab.*, **10**, 237 (1985).
4. J. A. Howard and J. H. B. Chenier, *Can. J. Chem.*, **54**, 390 (1976); **54**, 382 (1976).
5. K. B. Chakraborty, G. Scott, and W. R. Poyner, *Plast. Rubber Process. Appl.*, **3**, 59, (1983).
6. D. Gilead and G. Scott, in *Developments in Polymer Stabilization*—5, G. Scott, Ed., Applied Science, London, 1982, Chap. 4.
7. M. U. Amin and G. Scott, *Eur. Polym. J.*, **16**, 1019 (1974).
8. S. Al-Malaika, M. Coker, and G. Scott, *Polym. Deg. Stab.*, **10**, 173 (1985).
9. D. Gilead and G. Scott, Br. Pat. 1,586,344 (1978).
10. M. S. Kharasch, A. Fono, and W. Nudenburg, *J. Org. Chem.*, **16**, 113 (1951).
11. B. W. Evans and G. Scott, *Eur. Polym. J.*, **10**, 453 (1974).
12. S. Al-Malaika and G. Scott, *Eur. Polym. J.*, **16**, 503 (1980).
13. L. A. Brooks, *Rubber Chem. Tech.*, **36**, 887 (1963).
14. J. D. Holdsworth, G. Scott, and D. Williams, *J. Chem. Soc.*, **1964**, 4692.
15. M. J. Husbands and G. Scott, *Eur. Polym. J.*, **15**, 249 (1979).
16. S. Al-Malaika, K. B. Chakraborty, G. Scott, and Z. B. Tao, *Polym. Deg. Stab.*, **13**, 261 (1985).
17. V. G. Vinogradova and A. N. Zverev, *Izv. Akad. Nauk SSSR, Ser. Kim.*, **10**, 2217 (1975).

Received March 3, 1986

Accepted July 22, 1986